

Unquenched Kogut-Susskind quark propagator in Lattice Landau Gauge QCD

Sadataka Furui*

School of Science and Engineering, Teikyo University, 320-8551 Japan.

Hideo Nakajima†

Department of Information Science, Utsunomiya University, 321-8585 Japan.

(Dated: May 24, 2019)

Quark propagators of the unquenched Kogut-Susskind(KS) fermion obtained from the gauge configurations of the MILC collaboration are measured after Landau gauge fixing and using the Staple+Naik action. Presence of the $\bar{q}q$ condensates and A^2 condensates in the dynamical mass $M(q)$ and the quark wave function renormalization $Z_\psi(q^2)$ are investigated. We obtain the correlation of the renormalization factor of the running coupling taken at $\mu \sim 6\text{GeV}$ and that of the quark wave function renormalization $Z_\psi(q^2)$ of the Staple+Naik action. The mass function $M(q)$ is finite at $q = 0$ and its chiral limit is $\sim 0.36\text{GeV}$. We compared the results corrected by the scale of the vertex renormalization and the tadpole renormalization with the corresponding values obtained by the Asqtad action without renormalization and observed good agreement. Implication of infrared finite $Z_2(q) = 1/Z_\psi(q^2)$ to the Kugo-Ojima confinement criterion is discussed.

PACS numbers: 12.38.Gc, 12.38.Aw, 11.10.Gh, 11.15.Ha, 11.15.Tk, 11.30.Rd

I. INTRODUCTION

The mechanism of dynamical chiral symmetry breaking and confinement is one of the most fundamental problem of hadron physics. The propagator of dynamical quarks in the infrared region provides information on dynamical chiral symmetry breaking and confinement. In the previous paper[1], we measured gluon propagators and ghost propagators of unquenched gauge configurations obtained with quark actions of Wilson fermions (JLQCD/CP-PACS) and those of Kogut-Susskind(KS) fermions (MILC) in Landau gauge and observed that the configurations of the KS fermion are closer to the chiral limit than those of Wilson fermions.

In the analysis of running coupling obtained from the gluon propagator and the ghost propagator, with use of the operator product expansion of the Green function, we observed possible contribution of the quark condensates, A^2 condensates and gluon condensates in the configurations of the KS fermion[1]. The quark propagator of quenched KS fermion was already measured in [2], and possible contribution of these condensates are reported. Unquenched KS fermion propagator of $20^3 \times 64$ lattice (MILC_c) was measured in [6], but to distinguish the gluon condensates and the quark condensates, it is desirable to measure the quark propagator of larger lattice (MILC_f) and to compare with data of MILC_c. We measure quark propagator of gauge configuration produced by using the Asqtad action 1) MILC_c $20^3 \times 64$, $\beta = 6.76$ and 6.83 and 2) MILC_f $28^3 \times 96$, $\beta = 7.09$ and 7.11 . @

The paper is organized as follows. In sect.2 we present kinematics of the staggered fermion on the lattice, and in sect.3 the algorithm of the inversion to get the quark propagator is shown. In sect.4 we show the renormalization effects and in sect. 5 numerical results of the mass function and the quark propagator are presented. Finally in sect.6 we give conclusion and discussion.

II. KINEMATICS OF THE KS FERMION

The methods of writing the KS fermionic action on the lattice and deriving its propagator are presented in [3]. The KS fermion contains 16 flavor degrees of freedom and it is necessary to reduce the extra degrees of freedom by taking the 4th root of the fermion determinant. The MILC collaboration improved the fermionic action by fattening the gauge links, including Naik term and multiplying the tadpole renormalization factor so that the continuum limit can be approached on relatively small size of the lattice[4, 5]. Although there are no rigorous justification, there are indications that taking the 4th root does not yield serious problems.

In [6], a formulation of the KS fermion propagator calculation was presented and the numerical calculation was performed on MILC_c ($20^3 \times 64$ lattices) data[8]. In these papers, the momentum of quarks on the hypercubic lattice is defined by

$$p_\mu = \frac{2\pi n_\mu}{L} \quad (1)$$

where $n_\mu = 1, 2, \dots, L/4$ and the 16 flavor degrees of freedom $\alpha_\mu = 0, 1$ where $\mu = 1, \dots, 4$, are expressed as

$$k_\mu = p_\mu + \pi\alpha_\mu \quad (2)$$

*Electronic address: furui@umb.teikyo-u.ac.jp;
URL: http://albert.umb.teikyo-u.ac.jp/furui_lab/furuipbs.htm

†Electronic address: nakajima@is.utsunomiya-u.ac.jp

In the Asqtad action, the link variable is modified by fattening

$$U_{\mu}^{fat}(x) = c_1 U_{\mu}(x) + \sum_{\nu} [w_3 S_{\mu\nu}^{(3)}(x) + \sum_{\rho} (w_5 S_{\mu\nu\rho}^{(5)}(x) + \sum_{\tau} w_7 S_{\mu\nu\rho\tau}^{(7)}(x))] \quad (3)$$

where $S_{\mu\nu}^{(3)}$ is the staple contribution

$$S_{\mu\nu}^{(3)}(x) = U_{\nu}(x) U_{\mu}(x + \hat{\nu}) U_{\nu}^{\dagger}(x + \hat{\mu}) + h.c. \quad (4)$$

$S^{(5)}$ and $S^{(7)}$ are 5-link and 7-link contribution, respectively. In addition to fattening, so called Naik term and Lepage term are added. The Naik term is a product of three link variables along one direction[4].

$$U_{\mu}^{Naik}(x) = c_N U_{\mu}(x) U_{\mu}(x + \hat{\mu}) U_{\mu}(x + 2\hat{\mu}) \quad (5)$$

and the Lepage term is

$$U_{\mu}^{Lepage}(x) = c_L U_{\nu}(x) U_{\nu}(x + \hat{\nu}) U_{\mu}(x + 2\hat{\nu}) \times U_{\nu}^{\dagger}(x + \hat{\nu} + \hat{\mu}) U_{\nu}^{\dagger}(x + \hat{\mu}). \quad (6)$$

We compare the action including $S^{(3)}$ staple term and the Naik term only (Staple+Naik action), i.e. the same as that of [9], Asq action and Asqtad action.

The Staple+Naik action is

$$S_{\alpha\beta}^{-1}(x, y) = \sum_{\mu=-4}^4 \eta_{\mu}(x) \text{sign}(\mu) \times [(c_1 U_{\mu}(x) + w_3 \sum_{\nu \neq \mu} S_{\mu\nu}^{(3)}(x)) \delta_{y, x+\hat{\mu}} + c_N U_{\mu}^{Naik}(x) \delta_{y, x+3\hat{\mu}}] \quad (7)$$

where and $c_1 = 9/32$, $w_3 = 9/64$ and $c_N = -1/24$.

The Asq action contains $S^{(3)}$, $S^{(5)}$, $S^{(7)}$ and Lepage term and the Naik term but no tadpole renormalization factor.

$$S_{\alpha\beta}^{-1}(x, y) = \sum_{\mu=-4}^4 \eta_{\mu}(x) \text{sign}(\mu) \times [(c_1 U_{\mu}(x) + \sum_{\nu} w_3 S_{\mu\nu}^{(3)}(x) + \sum_{\rho} (w_5 S_{\mu\nu\rho}^{(5)}(x) + \sum_{\tau} w_7 S_{\mu\nu\rho\tau}^{(7)}(x)) + c_L U_{\mu}^{Lepage}(x)) \delta_{y, x+\mu} + c_N U_{\mu}^{Naik}(x) \delta_{y, x+3\mu}] \quad (8)$$

where $c_1 = 5/8$, $w_3 = 1/16$, $w_5 = 1/64$, $w_7 = 1/384$, $c_L = -1/16$ and $c_N = -1/24$.

The full Asqtad action contains the tadpole renormalization factor. Different from [5], we do not absorb one power of u_0 into the quark mass in our calculation of the quark propagator, and use $c_1 = 5/8 u_0^{-1}$, $w_3 = 1/16 u_0^{-3}$, $w_5 = 1/64 u_0^{-5}$, $w_7 = 1/384 u_0^{-7}$, $c_L = -1/16 u_0^{-5}$ and $c_N = -1/24 u_0^{-3}$.

The Dirac gamma function of KS fermions are defined as[6]

$$(\bar{\gamma}_{\mu})_{\alpha\beta} = (-1)^{\alpha\mu} \delta_{\alpha+\zeta^{(\mu)}, \beta} \quad (9)$$

where

$$\zeta_{\nu}^{(\mu)} = \begin{cases} 1 & \nu < \mu \\ 0 & \text{otherwise} \end{cases} \quad (10)$$

In momentum space the inverse propagator is expressed as

$$S_{\alpha\beta}^{-1}(p, m) = i \sum_{\mu} (\bar{\gamma}_{\mu})_{\alpha\beta} \left(\frac{9}{8} \sin p_{\mu} - \frac{1}{24} \sin 3p_{\mu} \right) + m \bar{\delta}_{\alpha\beta} \quad (11)$$

where

$$\bar{\delta}_{\alpha\beta} = \prod_{\mu} \delta_{\alpha_{\mu}\beta_{\mu}} \quad (12)$$

III. ALGORITHM FOR CALCULATING THE PROPAGATOR

The inversion of the $S_{\alpha\beta}^{-1}(x, y)$ is performed via conjugate gradient method after preconditioning[14] as follows.

We consider

$$\begin{aligned} \mathcal{D}_{\mu}(x, y) &= \frac{1}{2} \sum_{\mu=1, \dots, 4} \eta_{\mu}(x) \\ &\times \{ U_{\mu}^{fat}(x) \delta_{y, x+\mu} + U_{\mu}^{Naik}(x) \delta_{y, x+3\mu} \\ &- U_{\mu}^{fat}(x)^{\dagger} \delta_{y, x-\mu} - U_{\mu}^{Naik}(x)^{\dagger} \delta_{y, x-3\mu} \} \end{aligned} \quad (13)$$

We define the operator divided by the bare mass of the dynamical quark m as

$$\bar{M} = (I + \frac{1}{m} \mathcal{D}) \quad (14)$$

and decompose even sites and odd sites,

$$\bar{M} = \begin{pmatrix} I & \frac{1}{m} \mathcal{D}_{oe} \\ \frac{1}{m} \mathcal{D}_{eo} & I \end{pmatrix} = I - L - U \quad (15)$$

where

$$L = \begin{pmatrix} 0 & 0 \\ -\frac{1}{m} \mathcal{D}_{eo} & 0 \end{pmatrix} \quad (16)$$

and

$$U = \begin{pmatrix} 0 & -\frac{1}{m} \mathcal{D}_{oe} \\ 0 & 0 \end{pmatrix} \quad (17)$$

Using the Eisenstat trick, we define

$$\begin{aligned} \tilde{M} &= (I - L)^{-1} \bar{M} (I - U)^{-1} = (I + L)(I - U - L)(I + U) \\ &= I - LU = \begin{pmatrix} I & 0 \\ 0 & I - (\frac{1}{m})^2 \mathcal{D}_{eo} \mathcal{D}_{oe} \end{pmatrix} \end{aligned} \quad (18)$$

We note that \tilde{M} is hermitian and the conjugate gradient method and/or BiCGstab method are applicable.

With use of the definition

$$\frac{1}{m}\rho = \rho' = \begin{pmatrix} \rho'_o \\ \rho'_e \end{pmatrix} \quad (19)$$

and

$$\phi = \begin{pmatrix} \phi'_o \\ \phi'_e \end{pmatrix}, \quad (20)$$

we solve

$$(I - \frac{1}{m^2} \mathcal{D}_{eo} \mathcal{D}_{oe}) \tilde{\phi}_e = \rho'_e - \frac{1}{m} \mathcal{D} \rho'_o \quad (21)$$

with initial value $\tilde{\phi}_e^{(0)} = \tilde{\rho}'_e$. The odd site solution is $\tilde{\phi}_o = \rho'_o - \frac{\mathcal{D}}{m} \tilde{\phi}_e$.

The decomposition into even sites and odd sites is done by multiplying the projection operator P_e and P_o , and the color source ρ' is taken as a vector of 3×3 matrices.

The convergence condition for the conjugate gradient iterations is

$$\frac{\|\tilde{M}\phi - \rho\|}{\|\rho\|} < \text{a few per cent at most} \quad (22)$$

where the used norm is maximum norm in the space of site, color and flavor, and the accuracy gets 10^{-1} higher if L^2 norm is used.

$$S(q) = \mathcal{Z}_2(q) \frac{-i\not{q} + \mathcal{M}(q)}{q^2 + \mathcal{M}(q)^2} \quad (23)$$

Since $\text{tr} \gamma_\mu = 0$, tr over color and flavor yields

$$\begin{aligned} \text{tr} S(q) &= 16N_c \frac{\mathcal{Z}_2(q) \mathcal{M}(q)}{q^2 + \mathcal{M}(q)^2} \\ &= 16N_c \mathcal{B}(q) \end{aligned} \quad (24)$$

On the other hand

$$\begin{aligned} \text{tr}(i\not{q} S) &= \text{tr} \mathcal{Z}_2(q) \frac{q^2}{q^2 + \mathcal{M}(q)^2} \\ &= 16N_c q^2 \frac{\mathcal{Z}_2(q)}{q^2 + \mathcal{M}(q)^2} \\ &= 16N_c q^2 \mathcal{A}(q) \end{aligned} \quad (25)$$

The dynamical mass of the quark is

$$\mathcal{M}(q) = \frac{\mathcal{B}(q)}{\mathcal{A}(q)} \quad (26)$$

and the quark wave function renormalization is

$$\mathcal{Z}_2(q) = \frac{\mathcal{A}(q)^2 q^2 + \mathcal{B}(q)^2}{\mathcal{A}(q)}. \quad (27)$$

IV. RENORMALIZATION EFFECTS

In the continuum theory, the quark wavefunction renormalization $Z_\psi(q^2)$ is defined by the renormalized inverse quark propagator $S^{-1}(q)$ as[12, 15]

$$S^{-1}(q) = \delta_{ab} Z_\psi(q^2) (i\not{q} + M(q)) \quad (28)$$

When the mass renormalization is taken into account, the renormalized quark propagator is given by the bare quark propagator S_0 as[11]

$$S_R(q, m_{ren}) = Z_\psi S_0(q, m_0)|_{m_0=m_{ren}/Z_m} \quad (29)$$

where, in the case of KS fermion, the conditions

$$\lim_{m_{ren} \rightarrow 0} -\frac{i}{16N_c} \text{tr} \left(\frac{\partial S_R^{-1}}{\partial \not{q}}(q) \right)_{q^2=\mu^2} = 1 \quad (30)$$

and

$$\lim_{m_{ren} \rightarrow 0} \frac{1}{16N_c m_{ren}} \text{tr} (S_R^{-1}(q))_{q^2=\mu^2} = 1 \quad (31)$$

fixes Z_ψ and Z_m .

On the lattice, we identify $Z_\psi(q^2)$ by

$$Z_\psi(q^2) = \frac{g_1(\mu^2) \mathcal{A}(q)}{\mathcal{A}(q)^2 q^2 + \mathcal{B}(q)^2} \quad (32)$$

The function $\mathcal{B}(q)$ defines the quark inverse propagator $Z_\psi(q)$ and the dynamical mass $M(q)$ as

$$\mathcal{B}(q) = \mathcal{A}(q) \mathcal{M}(q) \propto \frac{1}{Z_\psi(q^2)} M(q). \quad (33)$$

In the following, we identify $M(q) = \mathcal{M}(q)$ and renormalize the quark field as $\sqrt{Z_\psi} \psi_{bare} = \psi_R$.

The Ward identity implies that the wavefunction renormalization can be defined via conserved vector current vertex. We define the colorless vector current vertex by using[12]

$$G_\mu(q, p) = \int d^4x d^4y e^{iq \cdot y + ip \cdot x} \langle q(y) \bar{q}(x) \gamma_\mu q(x) \bar{q}(0) \rangle \quad (34)$$

and

$$\Gamma_\mu(q, p) = S^{-1}(q) G_\mu(p, q) S^{-1}(p + q) \quad (35)$$

The vertex of the vector current is written as

$$\begin{aligned} \Gamma_\mu(q) &= \delta_{a,b} \{ g_1(q^2) \gamma_\mu + i g_2(q^2) q_\mu + g_3(q^2) q_\mu \not{q} \\ &\quad + i g_4(q^2) [\gamma_\mu, \not{q}] \} \end{aligned} \quad (36)$$

The Ward identity in the renormalized form tells

$$(\Gamma_R)_\mu(q) = -i \frac{\partial}{\partial q^\mu} S_R^{-1}(q) \quad (37)$$

After multiplying both sides by Z_ψ , one obtains

$$Z_V \Gamma_\mu(q) = -i \frac{\partial}{\partial q^\mu} S^{-1}(q) \quad (38)$$

where $Z_V g_1(q^2) = Z_\psi(q^2)$ and $Z_V = 1$ in the continuum limit and $Z_\psi(q^2)/g_1(q^2) = Z_V^{MOM}(a^{-1}, q^2)$ is expected to be independent of q in the limit of $a^{-1} \rightarrow \infty$.

In the Schwinger-Dyson approach[7] the running coupling g of the ghost, anti-ghost, gluon coupling is

$$g(q) = \tilde{Z}_1 Z_3^{-1/2}(\mu^2, q^2) \tilde{Z}_3^{-1}(\mu^2, q^2) \quad (39)$$

and that of quark, gluon coupling is calculated as

$$g(q) = Z_1^\psi Z_3^{-1/2}(\mu^2, q^2) Z_2^{-1}(\mu^2, q^2). \quad (40)$$

At the renormalization point $q = \mu$, we fix $Z_2(\mu^2, \mu^2) = 1$ and $Z_3(\mu^2, \mu^2) = 1$, and thus

$$\tilde{Z}_1 \tilde{Z}_3^{-1} = Z_1^\psi Z_2^{-1} \quad (41)$$

i.e. $\tilde{Z}_1 = Z_1^\psi$. On the other hand

$$Z_1^\psi(q^2) = Z_V^{MOM} g_1(q^2) \quad (42)$$

where for 16 flavors

$$g_1(q^2) = \frac{1}{48N_c} \text{tr}[\Gamma_\mu(q, p=0)(\gamma_\mu - q_\mu \not{q})] \quad (43)$$

Since $Z_V^{MOM} = 1$ at the renormalization point, $g_1(\mu^2)$ is identical to $Z_1^\psi(\mu^2)$.

This expression suggests that the renormalization of Z_ψ on the lattice is defined by the renormalization of the running coupling on the lattice defined at $\mu \sim 6\text{GeV}$. We

TABLE I: The $1/\tilde{Z}_1^2$ factor of the unquenched SU(3).

config.	heavy	light	N_f	comments
MILC _c	1.49(11)	1.43(10)	3	$\beta_{imp} = 6.83, 6.76$
MILC _f	1.37(9)	1.41(12)	3	$\beta_{imp} = 7.11, 7.09$

define $Z_2(q^2) = 1/Z_\psi(q^2) = 1/Z_V g_1(\mu^2) = \mathcal{Z}_2(q)/g_1(\mu^2)$ and identify $1/g_1(\mu^2)$ for the Staple+Naik action as the average of the product of vertex renormalization factor and the tadpole renormalization factor i.e. $\tilde{Z}_1 u_0 = 1/1.38$ for MILC_c and $1/1.36$ for MILC_f.

In the case of Asq action, the renormalization factor $\mathcal{Z}_2(q)$ is suppressed by about 10% and the mass function $\mathcal{M}(q)$ is enhanced by about 10% as compared to the Staple+Naik. When the tadpole renormalization u_0 is included, i.e. in the case of Asqtad action, this change is compensated and the $Z_2(q^2)$ and $\mathcal{M}(q)$ become consistent with those of Staple+Naik action. In contrast to [8], we do not fix the scale of $\mathcal{Z}_2(q)$ of the Asqtad action at $q = 3\text{GeV}$ to be 1, but we use the bare lattice data $Z_2(q^2) = \mathcal{Z}_2(q)$. The $Z_2(q^2)$ and $\mathcal{M}(q)$ of Staple+Naik after the renormalization coincides with those of Asqtad action in the case of $m_0 = 82.2\text{MeV}$ as shown in Figs.1 and 2. In the case of $m_0 = 11.5\text{MeV}$, the $Z_2(q^2)$ and $\mathcal{M}(q)$ of Staple+Naik in the infrared region are shifted from those of Asqtad slightly, but the difference is about 10% at most.

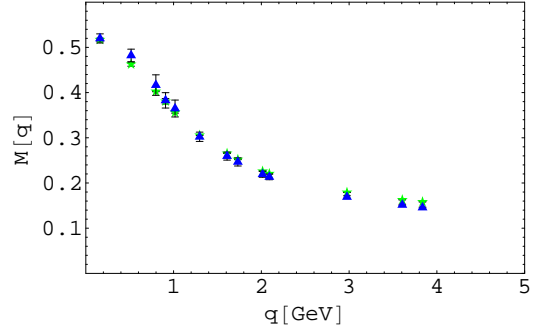


FIG. 1: The mass function $\mathcal{M}(q)$ of Staple+Naik action(stars) and the Asqtad action(triangles) of MILC_c with the bare quark mass $m_0 = 82.2\text{MeV}$.(Color online)

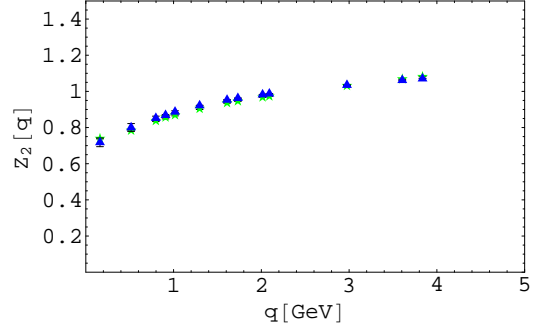


FIG. 2: The $Z_2(q^2)$ of Staple+Naik action(stars) and the Asqtad action(triangles) of MILC_c with the bare quark mass $m_0 = 82.2\text{MeV}$.(Color online)

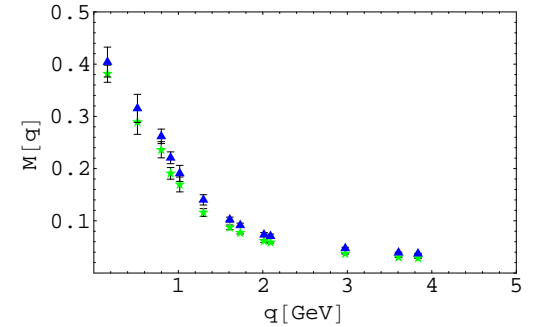


FIG. 3: The mass function $\mathcal{M}(q)$ of Staple+Naik action(stars) and the Asqtad action(triangles) of MILC_c with the bare quark mass $m_0 = 11.5\text{MeV}$.(Color online)

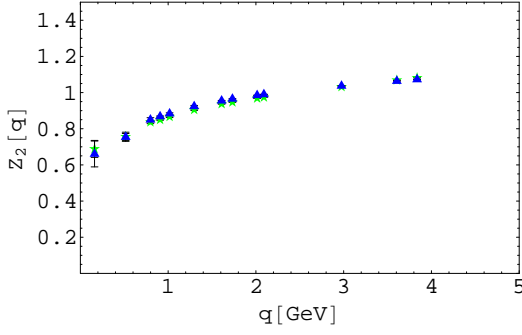


FIG. 4: The $Z_2(q^2)$ of Staple+Naik action(stars) and the Asqtad action(triangles) of MILC_c with the bare quark mass $m_0 = 11.5\text{MeV}$.(Color online)

V. ANALYSIS OF $M(q)$ AND $Z_\psi(q^2)$

In perturbative QCD (pQCD), dynamical mass of a quark is expressed as[2, 16, 17]

$$M(q) = -\frac{4\pi^2 d_M \langle \bar{q}q \rangle_\mu [\log(q^2/\Lambda_{QCD}^2)]^{d_M-1}}{3q^2 [\log(\mu^2/\Lambda_{QCD}^2)]^{d_M}} + \frac{m(\mu^2) [\log(\mu^2/\Lambda_{QCD}^2)]^{d_M}}{[\log(q^2/\Lambda_{QCD}^2)]^{d_M}}, \quad (44)$$

where $d_M = \frac{12}{33 - 2N_f}$. The second term is the contribution of the massive quark.

In this analysis of the lattice data, the quark condensates $-\langle \bar{q}q(\mu) \rangle$ and Λ_{QCD} are the fitting parameters. In the MILC_f lattice, the bare masses are $0.0062/a = 13.6\text{MeV}$ and $0.0124/a = 27.2\text{MeV}$ for the $u-d$ quarks and $0.031/a = 68.0\text{MeV}$ for the s -quark. In the MILC_c lattice, the corresponding masses are $0.007/a = 11.5\text{MeV}$ and $0.040/a = 65.7\text{MeV}$ for the $u-d$ quarks and $0.050/a = 82.2\text{MeV}$ for the s -quark.

The mass function eq.(44) is based on pQCD and cannot fit the data below 2GeV and we try the phenomenological fit[6, 26]

$$M(q) = \frac{c\Lambda^3}{q^2 + \Lambda^2} + m_0 \quad (45)$$

where m_0 is the bare quark mass. Parameters of c and Λ are summarized in TABLE II.

We observe that as the bare quark mass becomes heavy, c becomes smaller but the product $c\Lambda$ becomes larger. Although the MILC_c configurations of bare mass $m_0 = 82.2\text{MeV}$, with different β agree within errors, the MILC_f configurations of bare mass $m_0 = 68\text{MeV}$ show dependence on β . The mass function of $\beta = 7.09$ is smaller than that of $\beta = 7.11$. In the case of $\beta = 7.11$, the chiral limit $M(0)$ is consistent with that of MILC_c and we find $M(0)=0.37(1)\text{GeV}$. However, in the case of $\beta = 7.09$, $m_0 = 13.6\text{MeV}$, the lowest three momentum

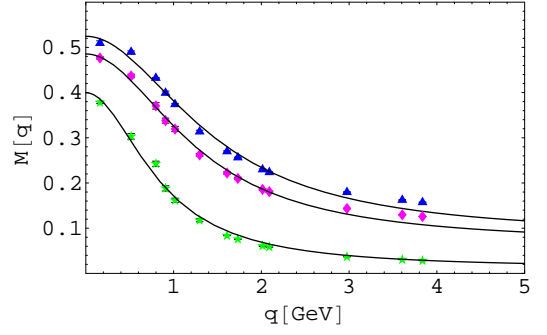


FIG. 5: The dynamical mass of the MILC_c quark (Staple+Naik) with bare mass $m_0 = 11.5\text{MeV}$ (stars), 65.7MeV (diamonds) and 82.2MeV (triangles) and the phenomenological fits. (Color online)

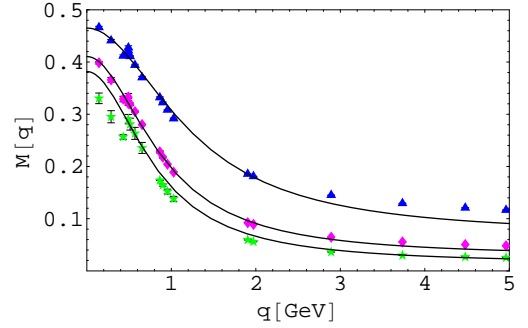


FIG. 6: Same as FIG. 5 but MILC_f quark with bare mass $m_0 = 13.6\text{MeV}$ (stars), 27.2MeV (diamonds) and 68.0MeV (triangles) and the phenomenological fits.(Color online)

points of $M(q)$ are systematically smaller than the other points. The slope of the $\beta = 7.09$ and that of 7.11 are almost the same. Hence we expect that the $M(0)$ in the continuum limit would be smaller than 0.36GeV .

We show the lattice results of $Z_2(q)$ of MILC_f and MILC_c in Figs. 8 and 9, respectively.

The apparent difference in the formulae of [8] and our

TABLE II: The parameters c and Λ .

β_{imp}	$m_0(\text{MeV})$	c	$\Lambda(\text{GeV})$	$c\Lambda(\text{GeV})$
6.76	11.5	0.44(1)	0.87(2)	0.383
	82.2	0.30(1)	1.45(2)	0.431
	65.7	0.33(1)	1.28(2)	0.420
6.83	82.2	0.30(1)	1.45(2)	0.431
	13.6	0.45(1)	0.82(2)	0.368
7.09	68.0	0.30(1)	1.27(4)	0.381
	27.2	0.43(1)	0.89(2)	0.383
7.11	68.0	0.32(1)	1.23(2)	0.397

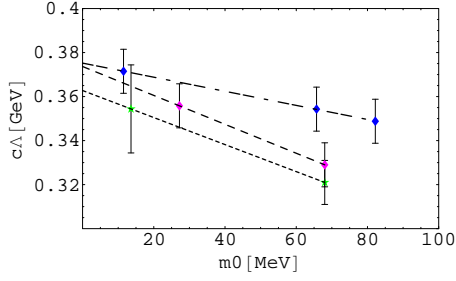


FIG. 7: The chiral symmetry breaking mass $c\Lambda = M(0) - m_0$ as a function of bare mass and its chiral limit. Dotted line is the extrapolation of MILC_f $\beta = 7.09$, dashed line is $\beta = 7.11$ and the dash-dotted line is that of MILC_c. (Color online)

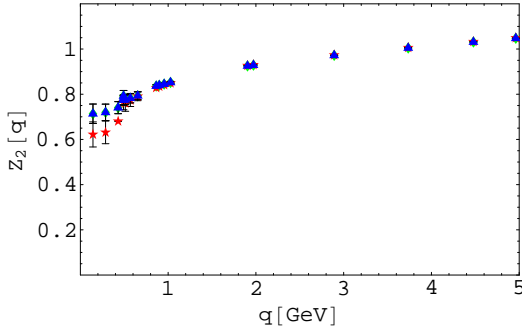


FIG. 8: The $Z_2(q^2)$ of MILC_f with bare mass $m_0 = 13.6\text{MeV}$ (stars), 27.2MeV (diamonds) and 68MeV (triangles). (Color online)

work are only in the expression and in fact they are equivalent. The $Z_2(q)$ agree with each other.

The $A(q)$ defined as $S(q) = \frac{1}{A(q)\not{q} - B(q)}$ is

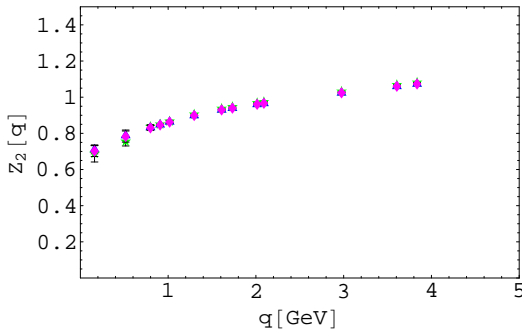


FIG. 9: Same as FIG. 8 but quark of MILC_c with bare mass $m_0 = 11.5\text{MeV}$ (stars), 65.7MeV (diamonds) and 82.2MeV (triangles). The last two almost overlap. (Color online)

parametrized in the OPE approach as[19]

$$A(q) = 1 + \frac{\pi\alpha_s(\mu^2)\langle A^2 \rangle_\mu}{N_c q^2} - \frac{\pi\alpha_s(\mu^2)\langle F^2 \rangle_\mu}{3N_c q^4} + \frac{3\pi\alpha_s(\mu^2)\langle \bar{q}gAq \rangle_\mu}{4q^4} \quad (46)$$

where $\langle F^2 \rangle_\mu$ is the gluon condensate, $\alpha_s(\mu^2)\langle A^2 \rangle_\mu$ is the A^2 condensate and $\langle \bar{q}gAq \rangle_\mu$ is the mixed condensate, which are the fitting parameters.

Similar parametrization was done by [2], in which $\mu = 2\text{GeV}$ and $A(q)$ for $q > 1\text{GeV}$ is parametrized as

$$A(q) = 1 + \frac{c_1}{q^2} + \frac{c_2}{q^4} \quad (47)$$

In this parametrization, we obtained $c_1 = 0.25\text{GeV}^2$, $c_2 = 0.061\text{GeV}^4$ in the case of $m_0 = 27\text{MeV}$. Comparing with data of quenched simulation[2] ($c_1 = 0.37 \pm 0.06\text{GeV}^2$ and $c_2 = -0.25 \pm 0.04\text{GeV}^4$), c_1 is the same order but c_2 is smaller and have opposite sign. The result depends on the choice of the renormalization point μ .

The pQCD result of the wave function renormalization factor $Z_2(q^2)$ in \overline{MS} scheme up to four loop is given by [22, 23]. Orsay group expanded the $\alpha_s^{\overline{MS}}$ in terms of $\alpha_s^{MOM}(q) = \alpha$ and obtained $Z_\psi^{pert}(q^2) = 1/Z_2(q^2)$ as a function of α and fitted the $Z_\psi(q^2)$ of Wilson overlap fermion in the \overline{MOM} scheme

$$\begin{aligned} (Z_\psi^{pert}(\mu^2))^{-1}S^{-1}(q) &= (Z_\psi^{pert}(\mu^2))^{-1}S_{pert}^{-1}(q) \\ &+ i\not{p} \frac{d(q^2/\mu^2, \alpha(\mu))}{q^2} \frac{\langle A^2 \rangle_\mu}{4(N_c^2 - 1)} \delta_{ab} + \dots \\ &= i\not{p} \delta_{ab} \left(\frac{Z_\psi^{pert}(q^2)}{Z_\psi^{pert}(\mu^2)} + \frac{d(q^2/\mu^2, \alpha(\mu))}{q^2} \frac{\langle A^2 \rangle_\mu}{4(N_c^2 - 1)} \right) \\ &+ \dots \end{aligned} \quad (48)$$

where $d(q^2/\mu^2, \alpha(\mu))$ is the solution of the renormalization group equation

$$\{(-\gamma_0 + \gamma_{A^2}^{(0)})\frac{\alpha(\mu)}{4\pi} + \frac{d}{d \log \mu^2}\} d(q^2/\mu^2, \alpha(\mu)) = 0 \quad (49)$$

which can be written as

$$d(q^2/\mu^2, \alpha(\mu)) = d(1, \alpha(q)) \left(\frac{\alpha(\mu)}{\alpha(q)} \right)^{(-\gamma_0 + \gamma_{A^2})/\beta_0} \quad (50)$$

The anomalous dimension of A^2 in the lowest order is[22, 25] $\gamma_{A^2}^{(0)} = \frac{35}{4} - \frac{2}{3}n_f$ and $\gamma_0 = 0$. We adopt $\langle A^2 \rangle$ as a fitting parameter and calculate

$$\begin{aligned} Z_\psi(q^2) &= \frac{g_1(\mu^2)}{Z_2(q^2)} \\ &= Z_\psi^{pert}(q^2) + \frac{\left(\frac{\alpha(\mu)}{\alpha(q)} \right)^{(-\gamma_0 + \gamma_{A^2})/\beta_0}}{q^2} \frac{\langle A^2 \rangle_\mu}{4(N_c^2 - 1)} Z_\psi^{pert}(\mu^2) \\ &+ \frac{c_2}{q^4} \end{aligned} \quad (51)$$

where $\alpha(q)$ are data calculated in the \widetilde{MOM} scheme using the same MILC_f gauge configuration[1].

We fitted the $Z_\psi(q^2)$ of MILC_f, $m = 27.2\text{MeV}$ data and choosing $\mu = 2\text{GeV}$ and $c_2 = 0$, obtained $\langle A^2 \rangle_\mu = 1.6(3)\text{GeV}^2$, which is compatible with the Orsay group data $2.4 \pm 0.3\text{GeV}^2$ for the Wilson fermion.

Definition of Z_ψ as the lattice data of $\frac{1}{Z_2}$ is subject to ambiguity due to the definition of the discretized lattice momentum[10] and the effect of spontaneous chiral symmetry breaking. The ratio of Z_ψ defined by eq.(29) and eq.(32) could deviate from 1 by about 40% in the infrared where the running coupling $\alpha_s(q^2)$ becomes about 2. Using the Ward identity, one could estimate Z_ψ from the vector current vertex $Z_\psi(q^2) = Z_V^{MOM} g_1(q^2)$, which is expected to behave as the running coupling $\alpha_s(q^2)$ in the infrared region.

In FIG.10, we show the lattice data of $Z_\psi(q^2) = \frac{g_1(\mu^2)}{Z_2(q)}$ from the Staple+Naik action with $g_1(\mu^2)=1.36$ i.e. the average of the running coupling renormalization factor of MILC_f in the previous analysis[1], and the phenomenological fit $Z_\psi^{fit}(q^2)$ by eq.(51). The pQCD result $Z_\psi^{pert}(q^2)$ above $q = 1\text{GeV}$ is shown by the dashed line and the lattice data of $\alpha_s(q)$ below $q = 0.5\text{GeV}$ obtained by the ghost anti-ghost gluon coupling are also plotted.

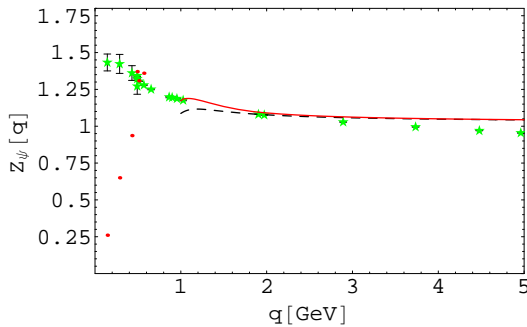


FIG. 10: The quark wave function renormalization $Z_\psi(q^2)$ of MILC_f bear mass $m_0 = 27.2\text{MeV}$. The solid line is the phenomenological fit as [12] and the dashed line is the pQCD result. The points below 0.6GeV are $g_1(q^2)$ approximated by the running coupling obtained by the ghost anti-ghost gluon vertex. (Color online)

The suppression of $Z_\psi(q^2)$ in the infrared suggested by the behavior of $\alpha_s(q)$ could be an artefact. In the case of Wilson fermion[11], the $Z_\psi(q^2)$ in the continuum limit is infrared finite.

VI. CONCLUSION AND DISCUSSION

We measured the quark propagator of the MILC_f lattice ($28^3 \times 96$) of $\beta_{imp} = 7.09$ and 7.11 and MILC_c lattice ($20^3 \times 64$) of $\beta_{imp} = 6.76$ and 6.83 using the Staple+Naik

action. After the renormalization using the information of the running coupling and the tadpole renormalization, we obtained a good agreement with the lattice bare data of the Asqtad action in the case of MILC_c.

We observed that the denominator of the quark renormalization factor

$$Z_2(q^2) = \frac{\mathcal{A}(q)^2 q^2 + \mathcal{B}(q)^2}{g_1(\mu^2) \mathcal{A}(q)} \quad (52)$$

is a steeply increasing function as q approaches 0 which causes the infrared suppression. Although the function $\mathcal{B}(q)$ in the numerator is also an increasing function of q as q approaches 0, it is almost constant as the bare mass m_0 decreases, in contrast to $\mathcal{A}(q)$ which becomes larger as the bare mass m_0 decreases.

The infrared feature of $Z_\psi(q^2) = \frac{1}{Z_2(q^2)}$ is related to the Kugo-Ojima color confinement criterion:

$$1 - c = \frac{Z_1}{Z_3} = \frac{\tilde{Z}_1}{\tilde{Z}_3} = \frac{Z_{1\psi}}{Z_2} = 0 \quad (53)$$

In the quark sector, divergence of $Z_2(q^2)$ or vanishing of $Z_\psi(q^2)$ in the infrared is consistent with the Kugo-Ojima confinement criterion. Infrared finiteness of Z_2 implies that $Z_{1\psi}$ is infrared vanishing, and infrared finite Z_ψ supports the idea that the running coupling freezes to a finite value in the infrared. This situation is similar to that of the gluon sector. The infrared finite lattice data of Z_3 implies that Z_1 is also infrared vanishing. In this case running coupling defined by (39) vanishes unless Z_3 is infrared vanishing. Definition of the running coupling from the triple gluon vertex is more ambiguous than the definition (40) from the ghost-gluon vertex, and we expect that the fluctuation of the ghost propagator in the infrared induces the artefacts in the infrared running coupling.

We compared the Staple+Naik action and the Asqtad action and found that the mass function and the quark propagator are consistent with each other. They are consistent with the results of other group[6, 8, 28].

We confirmed A^2 condensates which was found by the Orsay group in the running coupling of quenched lattice simulation[27] and observed in the unquenched lattice simulation[1, 12] also in the quark propagator. We observed also the indication of the $\bar{q}q$ condensate.

The effect of dynamical chiral symmetry breaking is seen in the mass function $M(q)$. By extrapolation to the chiral limit we obtain $M(0) \sim 0.36\text{GeV}$, which is about 20% larger than [8].

Calculation of the quark propagator of MILC_f using the Asqtad action is underway and will be published in the future.

Acknowledgments

We thank Tony Williams and Patrick Bowman for helpful informations. Thanks are also due to MILC col-

laboration for the supply of their gauge configurations in the ILDG data base. This work is supported by the KEK supercomputing project 05-128. H.N. is supported

by the JSPS grant in aid of scientific research in priority area No.13135210.

-
- [1] S. Furui and H. Nakajima, hep-lat/0503029.
 - [2] E.R. Arriola, P.O. Bowman and W. Broniowski, hep-ph/0408309 v3
 - [3] H. Kluberg-Stern, A. Morel, O. Napoly and B. Petersson, Nucl. Phys. **B**[FS8],447(1983).
 - [4] C. Bernard et al., Phys. Rev. D**58**,014503(1998).
 - [5] K. Orginos, D. Toussaint and R.L. Sugar, Phys. Rev. D **60**,054503(1999).
 - [6] P.O. Bowman, U.M. Heller and A.G. Williams, Phys. Rev. D**66**,014505(2002).
 - [7] L. von Smecal, A. Hauck and R. Alkofer, Ann. Phys. (N.Y.) **267**,1(1998).
 - [8] P.O. Bowman, U.M. Heller, D.B. Leinweber, A.G. Williams and J.B. Zhang, Phys. Rev. D**71**,054507(2005).
 - [9] K. Orginos and D. Toussaint, Nucl. Phys. **B**(Proc. Suppl.)**73**,909(1999)
 - [10] E. Franco and V. Lubicz, Nucl. Phys. **B531**,641(1998).
 - [11] T. Blum et al., Phys. Rev. D**66**,014504(2002).
 - [12] Ph. Boucaud, F. de Soto, A. Le Yaouanc, J. Micheli, H. Moutarde, O. Pène and J. Rodríguez-Quintero, hep-lat/0504017
 - [13] D. Becirević and V. Lubicz, hep-ph/0403044 v2
 - [14] S. Fischer, A. Frommer, U. Glaässer, Th. Lippert, G. Litzenhöfer and K. Schilling, Comp. Phys. Comm. **98**,20(1996).
 - [15] H. Pagels, Phys. Rev. D**19**,3080(1979).
 - [16] K.D. Lane, Phys. Rev. D**10**,2605(1974).
 - [17] H.D. Politzer, Nucl. Phys. **B117**,397,(1976).
 - [18] J. Ahlback, M.J. Lavelle, M. Shaden and A. Streibl, Phys. Lett. B**275**,124(1992).
 - [19] M.J. Lavelle and M. Oleszczuk, Phys. Lett. B**275**,133(1992).
 - [20] C. McNeile, hep-lat/0504006.
 - [21] J.C.R. Bloch, Few Body Syst **33**,111(2003).
 - [22] K.G. Chetyrkin, hep-ph/0405193 v3(2005).
 - [23] K.G. Chetyrkin and A. Rétaý, arXiv:hep-ph/0007088; idem Nucl. Phys. **B583**,3(2000),arXiv:hep-ph/9910332.
 - [24] H. Vershelde, K. Knecht, K. Van Acoleyen and M. Vanderkelen, Phys. Lett. B**516**,307(2001),arXiv:hep-th/015018.
 - [25] D. Dudal, H. Vershelde and S.P. Sorella, Phys. Lett. B**155**,126(2003), hep-th/0212182.
 - [26] J.I. Skullerud and A.G. Williams, Phys. Rev. D**63**,054508(2001).
 - [27] P. Boucaud et al., JHEP **0004**, 006(2000), arXiv:hep-ph/003020.
 - [28] M.B. Parappilly, P.O. Bowman, U.M. Heller, D.B. Leinweber, A.G. Willioams and J.B. Zhang, hep-lat/0511007.